Radiol Oncol 1998; 32(1): 7–17

review

Digression on membrane electroporation and electroporative delivery of drugs and genes

Eberhard Neumann and Sergej Kakorin

Physical and Biophysical Chemistry, Faculty of Chemistry, University of Bielefeld, Germany

Introduction

A new kind of cell surgery has recently been developed by a combination of drugs and genes with electric voltage pulses. The novel surgery operates on the level of the cell membrane and uses membrane electroporation as a scalpel to greatly facilitate the penetration of drugs, especially chemotherapeuticals and genes through electroporated membrane patches of a cell.

The phenomenon of membrane electroporation (ME) is methodologically an electric technique which renders lipid membranes porous and permeable, transiently and reversibly, by external high voltage pulses. It is of practical importance that the *primary* structural changes induced by ME, condition the electroporated membrane for a variety of *secondary* processes such as, for instance, the permeation of otherwise impermeable substances.

The *structural* concept of ME was derived from *functional* changes; explicitly from the electrically induced permeability changes, indirectly judged from the partial release of intracellular components[1] or from the uptake of macromolecules such as DNA.[2,3] The electrically facilitated uptake of foreign genes is called the direct electroporative gene transfer or electrotransformation of cells. Similarly, electrofusion of single cells to large syncytia[4] and electroinsertion of foreign membrane proteins[5] into electroporated membranes are based on electrically induced structural changes of ME.

For the time being the method of ME is widely used to manipulate all kinds of cells, organelles and even intact tissue. ME is applied to enhance iontophoretic drug transport through skin, see, e.g., Pliquett et al.[6] , or to introduce chemotherapeuticals into cancer tissue, an approach pioneered by L. Mir.[7]

It is fair to say that, despite the attractive features of the various ME phenomena, the details of the molecular mechanism of ME itself are not yet known. On the same line, the mechanisms of various secondary processes coupled to ME have not been clarified yet. Therefore, reliable directives can not be given for specific analytical and cell-manipulative applications. However, model studies on cells and lipid vesicles have provided some insight into guidelines for the planning

Key words: membrane electroporation; gene transfer; drug delivery; lipid vesicle

Correspondence to: Prof Eberhard Neumann, Physical and Biophysical Chemistry, Faculty of Chemistry, University of Bielefeld, P. O. Box 100 131, D-33501 Bielefeld, Germany, Fax: +49 521 106 29 81; E–mail: eberhard.neuman@post.uni-bielefeld.de

of trials and for the optimization of existing procedures.

In this review a few fundamental aspects are selected which are important to consider when ME is to be applied to cells and tissue. We shall discuss some details of electric field induced structural changes leading to chemically specific pore states in the membrane (Figure 1). The rigorous thermodynamic and kinetic analysis of electroporation data shows that the structural changes increase *continuously* by time and electric field strength. Massive permeability changes, for instance reflected in large conductivity changes, or release and uptake of larger molecules are, however, associated with threshold field strengths (Figure 2) and delay times. Furthermore, the transport of drug-like dyes and DNA through electroporated membranes is characterized by transient interaction of the permeants with larger, but occluded, pores during the permeation process.

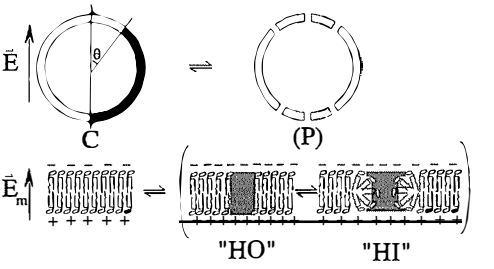

Figure 1. Chemical state transitions for the lipid rearrangements in the pore edges of the lipid vesicle membrane. Water entrance in the membrane is induced by an electric field causing the ionic interfacial polarization analogous to condenser plates (+, –), where θ is the polar angle. E is the externally applied field and E_m the induced membrane field. C denotes the closed bilayer state and (P) the porous state of hydrophobic (HO) and hydrophilic (HI) pores.

Why model systems?

Clearly, a goal-directed application of ME to cells and tissue requires knowledge of the molecular mechanisms. Due to the enormous complexity of cellular membranes, however, many fundamental problems of ME have to be studied at first on a simpler level of model membranes, such as lipid bilayer membranes or unilamellar lipid vesicles. When the primary processes are physico-chemically understood, the specific electroporative properties of real cell membranes and living tissue can also be quantitatively rationalized.

Membrane curvature

The importance of membrane curvature for ME in the context of protein adsorption and partial surface insertion has been studied with vesicles of different size, i.e., for different curvatures. Electrooptical studies using optical membrane probes like lipid-coupled 1,6 diphenyl-1,3,5-hexatriene (β-DPH-lipid) showed that an increased curvature (smaller vesicle radius) facilitates the electric pore formation. This observation was quantified[8] in terms of the energy content resulting from the different packing density of the lipid molecules in the two membrane leaflets of curved membranes; see, e.g., Seifert and Lipowsky[9] and references cited therein.

Electrolyte concentration

The importance of the electrolyte contents on both sides of membranes with charged lipids has become apparent when salt-filled vesicles were investigated. Different electrolyte concentrations cause different charge screening. The effect of this difference is theoretically described in terms of an increase in the membrane spontaneous curvature. Large concentration gradients across charged membranes of small vesicles permit electroporative efflux of electrolyte ions at surprisingly low transmembrane potential differences, for instance $|\Delta\varphi| = 37.5$ mV at a vesicle radius of a = 50 nm and pulse durations of $t_E = 100$ ms [10] compared with $|\Delta\varphi| \approx 500$ mV for planar (i.e., not curved) membranes.[11]

The pore concept – more than just semantics

No doubt, the various electroporative transport phenomena of release and uptake of substances clearly reflect transient permeability changes ultimately caused by external voltage pulses.[12,13] Membrane permeability changes and other electroporative secondary phenomena, however, result from field-induced structural changes in the membrane phase, leading to transient, yet long-lived permeation sites, pathways, channels or pores.[3,14,15]

Hydrophilic pores

Interestingly, field-induced penetration of small ions, of drug-like dyes and even the highly charged polyelectrolyte DNA, is also observed in the after-field time period, i.e. in the absence of the electrodiffusive driving force. Therefore, the electrically induced permeation sites must be polarized and specifically ordered, local structures which are potentially open for diffusion of permeantes. These local structures of lipids are long-lived (milliseconds to seconds) compared to the field pulse durations (typically 10 μs to 10 ms). Thus, the local permeation structures may be safely called transient pores or electropores in model membranes as well as in the lipid part of cell membranes. The special structural order of a long-lived pore may be modeled by the so-called inverted or hydrophilic (HI) pore (Figure 1).[16] On the same line, the massive ion transport through planar membranes, as observed in the dramatic conductivity increase when a voltage (≥ 100 – 500 mV) is applied, can hardly be rationalized without field-induced open passages or pores; see, e.g., the review by Weaver and Chizmadzhev.[15]

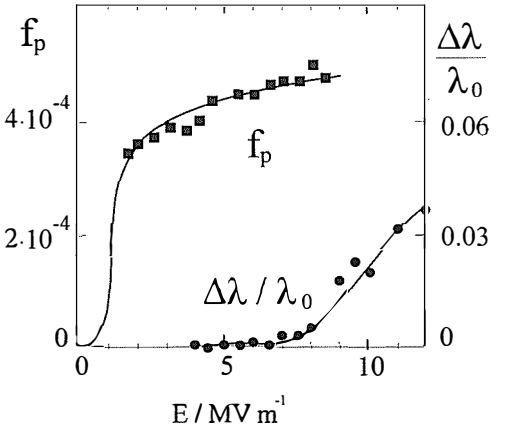

Figure 2. The fraction of the electroporated membrane area f_p smoothly increases with the field strength E, whereas the massive conductivity increase ($\Delta\lambda / \lambda_0$) of the suspension of the salt filled vesicles of radius a = 160 ± 30 nm indicates an apparent threshold value. The ratio $f_p = S_p / S_p^0$ was calculated from the electrooptic relaxations, yielding characteristic rate parameters of the electroporation – resealing cycle in its coupling to ion transport. Data from Neumann and Kakorin[16]: $\lambda_0 = 7.5$ μScm^{-1}, T = 293 K (20°C).

Attempts of pore visualization

Nevertheless, visible evidence for small electropores, such as electromicrographs, is not available. But the permeation of a permeant through an electroporated membrane patch has also not been visualized up to now. The large pore-like crater structures or volcanoes of 50 nm to 0.1 μm diameter, observed in electroporated red blood cells, most probably result from specific membrane-cytoskeleton interactions.[12] Voltage-sensitive fluorescence microscopy at the membrane level has shown that the transmembrane potential in the pole caps of sea urchin eggs is largely decreased, indicating that there the ionic conductivity of the membrane is increased, providing evidence for electropores.[13]

Born energy and transport

Membrane electropermeabilization for small ions and larger ionic molecules can not be simply described by a permeation across the densely packed lipids of an electrically modified membrane.[14] Theoretically, a small ion

such as $Na^+(aq)$ of 0.4 nm diameter and of charge $e = 1.6\times10^{-19}$ C, passing through a lipid membrane of 5 nm thickness encounters the Born energy barrier of $\Delta W_{Born} \approx 65$ kT, where $kT \approx 4.14\times10^{-21}$ J. Hence, the required transmembrane voltage to overcome this barrier amounts to 1.7 V. An even larger voltage of 7 V would be needed for divalent ions such as Ca^{2+} or Mg^{2+}. Nevertheless, the transmembrane potential required to electroporate the cell membrane usually does not exceed 0.5 V.[15] The reduction of the energy barrier can be readily achieved by a transient aqueous pore, which is the structural basis of the theory of electroporation. Certainly, the stationary open electropores can only be small (about 1 nm diameter) in order to prevent discharging of the membrane interface by ion conduction.[15,16] Because of the small size, these electropores can not be observed directly by electron microscopy. In any case, there appears to be no alternative to aqueous pores to rationalize the transport of ions and molecules through the electroporated membrane.[14]

Electrochemical thermodynamics of pore formation

Undoubtedly, the field-induced structural change leading to an aqueous pore in the lipid phase of the membrane is a chemical process promoted in the electric force field. The actual membrane field E_m is enormously amplified by interfacial polarization caused by the external field E[16], see below. In E, the redistribution of charges in the electrolyte solution adjacent to the membrane results in a charge distribution which is equivalent to condenser plates, the membrane being the dielectrics. However, unlike conventional solid state dielectrics, the lipid membrane is a highly dynamic phase of *mobile* lipid molecules in contact with *mobile* water molecules; the lipid membrane is hydrophobically kept together by the aqueous environment. Such a charged condenser with both mobile interior and mobile environment favors the entrance of water molecules to produce localized cross-membrane pores (P) with higher dielectric constant $\varepsilon_W \approx 80$ compared with $\varepsilon_L \approx 2$ of the replaced lipids (state C). In this sense, the lipid membrane in electrolyte solutions is an open system with respect to H_2O molecules, and surplus ions, charging the condenser in the presence of an external field[16].

The electrochemical model for the electroporation-resealing cycle

Chemically, the field-induced cycle of pore formation and resealing, after the electric field is switched off at the end of a pulse, can be viewed as a state transition from the intact closed lipid state (C) to the porous state (P) according to the reaction scheme:

$$C \underset{k_{-1}}{\overset{k_1}{\rightleftharpoons}} P \qquad (1)$$

The state transition involves a cooperative cluster (L_n) of n lipids L forming an electropore.[16,17] The extent of membrane electroporation y is defined by the concentration ratio

$$y = \frac{[P]}{[P] + [C]} = \frac{K}{1 + K} \qquad (2)$$

where $K = [P]/[C] = k_1/k_{-1}$ is the equilibrium distribution constant, k_1 the rate coefficient for the step $C \rightarrow P$ and k_{-1} the rate coefficient for the resealing step ($C \leftarrow P$). In an external electric field, the distribution in Eq. (1) is shifted in the direction of increasing [P] or, expressed differently, from $y[0] << 1$ at $E = 0$ to y(E) at E. Note that, for the frequently encountered observation of very small pore densities (see Figure 2), i.e., $K << 1$, Eq. (2) yields $y = f_p \approx K$. Hence the thermodynamic, field-dependent quantity K is directly obtained from the experimental degree of poration.

Kinetically, the reaction rate equation for the time course of the electroporation-resealing cycle reads:

$$\frac{d[P]}{dt} = -\frac{d[C]}{dt} = k_1[C] - k_{-1}[P] \qquad (3)$$

Mass conservation dictates that the total concentration is $[C_0] = [P] + [C]$. Substitution into Eq. (3) and integration yield the time course of pore formation:

$$[P(t)] = [C_0] \cdot \frac{K}{1+K}\left(1 - e^{-t/\tau}\right) \qquad (4)$$

where $[P_\infty] = [C_0]\, K / (1+K)$ is the amplitude of the relaxation process and

$$\tau = (k_1 + k_{-1})^{-1} = [k_{-1}(1+K)]^{-1} \qquad (5)$$

is the relaxation time or mean poration time. It is readily seen that from the experimentally accessible quantities τ and K, both rate coefficients, k_1 and k_{-1}, can be determined.

The symbol P may include several different pore states. If, for instance, we have to describe the pore formation by the sequence C = HO = HI, then (P) represents the equilibrium HO = HI between hydrophobic (HO) and hydrophilic (HI) pore states, see Figure 1, and a normal mode analysis is required.[17]

Energetics of membrane electroporation

The molar work energy difference $\Delta G_m = G_m(P) - G_m(C)$ between the two states C and P in the presence of an electric field must be expressed in terms of the standard value $\Delta_r\hat{G}^o$ of the transformed Gibbs reaction energy ($\hat{G}$) in order to relate the energetics to K.

Straightforward thermodynamics[18] yields

$$\Delta_r\hat{G}^o = -RT\, ln\, K \qquad (6)$$

where $R = N_A k_B$ is the gas constant, k_B the Boltzmann constant and N_A the Avogadro constant.

The difference term $\Delta_r\hat{G}^o$, or equivalently *l*n K, is generally the sum of chemical and physical contributions[16]:

$$\Delta_r\hat{G}^o = \Delta_r\hat{G}^o - \int\Delta_r M dE_m + \int\Delta_r\gamma dL + \int\Delta_r\Gamma dS + \int\Delta_r\beta dH \qquad (7)$$

Note that $\Delta_r = d/d\xi$, where ξ is the molar advancement of a state transition. Here $\Delta_r\hat{G}^o$ is the chemical contribution, $\int\Delta_r M dE_m$ the molar electric polarization term, $\int\Delta_r\gamma dL$ the molar pore edge energy, $\int\Delta_r\Gamma dS$ the molar pore surface energy term, $\int\Delta_r\beta dH$ the molar curvature energy term. The single terms are separately considered as follows:

Chemical contribution

The pure concentration changes of the lipid and water molecules involved in the formation of an aqueous pore with edges are covered by the conventional standard value $\Delta_r G^o = \sum_\alpha \sum_j \nu_j^\alpha \mu_j^{0,\alpha}$ of the Gibbs reaction energy, where ν_j^α and $\mu_j^{0,\alpha}$ are the stoichiometric coefficient and the standard chemical potential of the participating molecule J, respectively, constituting the phase α, i.e. either state C or state P. Here, $\Delta_r G^0 = \left(\mu_w^0 + \mu_L^0\right)_P - \left(\mu_w^0 + \mu_L^0\right)_C$.

Electric polarization term

The electric reaction moment $\Delta_r M = M_m(P) - M_m(C)$ in the electric polarization term $\int\Delta_r M\, dE_m$ refers to the difference in the molar dipole moments M_m of state C and P, respectively.

The field-induced reaction moment in the electrochemical model is given by[17]:

$$\Delta_r M = N_A \cdot V_p \cdot \Delta_r P \qquad (8)$$

where $V_p = \pi r_p \cdot d$ is the (induced) pore volume of the assumed cylindrical pore of

radius r_p and $d \approx 5$ nm is the dielectric membrane thickness.

Analogous with the physical analysis by Abidor et al.,[19] the reaction polarization is defined as:

$$\Delta_r P = \varepsilon_0(\varepsilon_W - \varepsilon_L)\, E_m, \qquad (9)$$

where ε_0 is the dielectric vacuum permittivity. The difference $\varepsilon_W - \varepsilon_L$ in the dielectric constants of water ε_W (20°C) = 80.4 and of lipids ε_L = 2.1 refers to the replacement of lipids by water. Since $\varepsilon_W >> \varepsilon_L$, the formation of aqueous pores is strongly favored in the presence of a cross-membrane potential difference $\Delta\varphi_m$ induced by the interfacial Maxwell-Wagner polarization. We use here the approximation $E_m = -\Delta\varphi_m/d$ for the membrane field valid for the small pores of low conductance.[15]

The stationary value of the induced potential difference $\Delta\varphi_m$ in the spherical membrane of a vesicle of radius a is dependent on the positional angle θ between the membrane site considered and the direction of the external field vector E (Figure 1):

$$\Delta\varphi_m = -\frac{3}{2} a \cdot E \cdot f(\lambda_m)\left|\cos\theta\right| \qquad (10)$$

The conductivity factor (λ_m) can be generally expressed in terms of a and d and the conductivities λ_m, λ_i, λ_0 of the membrane, the cell (vesicle) interior and the external solution, respectively.[20] Commonly, d << a and $\lambda_m << \lambda_0$, λ_i such that $f(\lambda_m) = [1 + \lambda_m (2 + \lambda_i / \lambda_0) / (2\, \lambda_i\, d/a)]^{-1}$. For $\lambda_m \approx 0$, $f(\lambda_m) = 1$. It is readily seen from Eq. (10) that the field amplification is quantified as $E_m = -\Delta\varphi_m / d = (3/2)(a/d) \cdot E \cdot f(\lambda_m)\left|\cos\theta\right|$, where the ratio a / d is the geometric amplification factor of interfacial membrane polarization.

The final expression of the electrical energy term (at θ) is obtained by sequential insertions and integration of Eq. (8). Explicitly[16,17],

$$\int_0^{E_m} \Delta_r M\, dE_m = \qquad (11)$$

$$= \frac{9\pi\varepsilon_0 \cdot a^2 \cdot (\varepsilon_W - \varepsilon_L) \cdot r_p^2 \cdot N_A}{8 \cdot d} f^2(\lambda_m) \cdot \cos^2\theta \cdot E^2$$

where we see that the polarization energy depends on the square of the field strength.

If the relation between K and E can be formulated as $K = K_0 \cdot \exp\left[\int \Delta_r\, M dE_m / RT\right]$, where K_0 refers to E = 0, Eq. (11) can be used to obtain the mean pore radius r_p from the field dependence of K or of y (the degree of poration).

We recall that the actual data always reflect θ angle averages (Figure 1).[17] Since [P] defines a surface area $S_p = N_p \cdot \pi r_p^2$ of N_p pores with maximally $S_p^0 = N_p \cdot \pi \cdot r_p^2$, the fraction of porated area is given by

$$f_p = \frac{[P]}{[P_{max}]} = \frac{S_p}{S_p^0} = \frac{1}{2}\int_0^{\pi} \frac{K(\theta)}{1 + K(\theta)} \sin\theta\, d\theta \qquad (12)$$

where f_p is the θ-average of $y = K(\theta) / (1 + K(\theta))$, with $[P_{max}] = [C_0]$. It is found that f_p is usually very small[21], e.g., $f_p \leq 0.003$, i.e. 0.3%. This value certainly corresponds to a small pore density, reguired for a low value of λ_m.

Curvature energy term

The explicit expression for the curvature energy term of vesicles of radius a is given by:[16]

$$\int \Delta_r \beta\, dH = N_A \int (\beta_P - \beta_C)\, dH \approx$$

$$\approx -\frac{64 \cdot N_A \cdot \pi^2 \alpha \cdot \kappa \cdot r_p^2 \cdot \zeta}{d} \cdot \left(\frac{1}{a} + \frac{H_0^{el}}{2\pi\alpha}\right) \qquad (13)$$

Note that the aqueous pore part has no curvature, hence the curvature term is $\beta_P - \beta_C = -\beta_C$. H is the curvature inclusively the spontaneous curvature H_0. If $H_0 = 0$, then in the case of spherical vesicles we have $H = 1/a$. H_0^{el} is the electrical part of the spontaneous curvature[16], κ is the elastic module, α is a material constant, ζ is a geometric fac-

tor characterizing the pore conicity.[9] It is noted that the molar curvature term $\int \Delta_r \beta \, dH$ can be as large as 10 RT.[8] Therefore, for small vesicles or small organelles and cells, the curvature term is very important for the energetics of ME.

Eq. (13) shows that the larger the curvature and the larger the H_0^{el} term, the larger is the energetically favorable release of Gibbs energy during pore formation. Strongly curved membranes appear to be electroporated easier than planar membrane parts.

Pore edge energy and surface tension

In Eq. (7), γ is the line tension or pore edge energy density and L is the edge length, Γ is the surface energy density and S is the pore surface in the surface plane of the membrane. Explicitly, for cylindrical pores we obtain the pore edge energy term:

$$\int_0^L \Delta_r \gamma \, dL = N_A \int_0^L (\gamma_P - \gamma_C) dL = 2\pi N_A \cdot \gamma \cdot r_p \quad (14)$$

where $\gamma_P = \gamma$ since $\gamma_C = 0$ (no edge) and $L = 2\pi r_p$ is the circumference line.

The surface pressure term

$$\int \Delta_r \Gamma \, dS = N_A \int_0^S (\Gamma_P - \Gamma_C) \, dS \quad (15)$$

is usually negligibly small because the difference in Γ between the states P and C is in the order of ≤ 1 mNm^{-1}; see, e.g., Steiner and Adam[22].

We recall that the conventional chemical term covering concentration changes of lipids and water in the pore edge and pore volume is given by $\Delta_r G^0 = -RT \ln K_0$. Applying this relation and Eqs. (11) – (14) to Eq. (6), we obtain the explicit expression:

$$K = K_0 \cdot \exp\left[-\frac{N_A}{RT} \left\{ 2\pi r_p \cdot \gamma - \beta \cdot \left(\frac{1}{a} + \frac{H_U^{el}}{2\pi\alpha} \right) \right\} + \frac{\int \Delta_r M \, dE_m}{RT} \right] \quad (16)$$

Experimentally, K can be determined from the fraction y of the porated surface as a function of the field strength. It remarked that K is exponentially dependent on the square of E, see Eq. (11). Therefore, the dependence of K or y on E is much stronger than linear such that the plot of y or f_p versus E (see Figure 2) shows an initial part of almost no change in y. This "lag phase" is very frequently qualified to indicate a threshold of the field strength. The thermodynamic analysis shows that ME is highly non-linear, yet continuous in E. Thus the structural aspect inherent in our membrane electroporation model is not associated with a threshold of the field strength. However, the pore density necessary to permit a secondary phenomenon such as massive ion conduction, release and uptake of substances, may very well be operationally described in terms of a threshold field strength (Figure 2).

The chemical thermodynamical concept has turned out to be applicable to the analysis of ME of vesicles, cells and organelles. For instance, it has been found that the stationary value of the mean pore radius within the pulse duration of 10 µs is rather small: $\bar{r}_p = 0.35 \pm 0.05$ nm, just permitting free passage of small ions.[17] At higher field intensities and longer pulse durations the pore radius may increase up to $\bar{r}_p \leq 1.2$ nm, leading to the influx of large drug-like dye molecules into the cell interior,[23] see below.

Electroporative cell deformations

Using lipid vesicles filled with electrolyte as a model for cells and organelles, it has been shown that ME is causing appreciable increases in the rate and extent of electromechanical shape deformations[10,21]. The overall shape deformation under the field-induced Maxwell stress is associated with several kinetically distinct phases. In the case of vesicles, the initial very rapid phase in the µs time range is the electroporative elonga-

tion from the spherical shape to an ellipsoid in the direction of the field vector E. In this phase, called phase 0 (Figure 3), there is no measurable release of salt ions, hence the internal volume of the vesicle remains constant. Elongation is therefore only possible if, in the absence of membrane undulations in small vesicles, the membrane surface can increase by ME. The formation of aqueous pores means entrance of water and increase in the membrane surface.

In the second, slower phase (ms time range), called phase I (Figure 3), there is efflux of salt ions under Maxwell stress through the electropores created in phase 0, leading to a decrease in the vesicle volume under practically constant membrane surface (including the surfaces of the aqueous pores). The kinetic analysis of the volume decrease yields the membrane bending rigidity $\kappa = 3.0 \pm 0.3 \times 10^{-20}$ J.[21] At the field strength E = 1.0 MV m^{-1} and in the range of pulse duration $5 \leq t_E/\text{ms} \leq 60$, the number of water-permeable electropores is found to be $N_p = 35 \pm 5$ per vesicle of radius a = 50 nm, with mean pore radius $\bar{r}_p = 0.9 \pm 0.1$ nm.

The kinetic analysis developed for vesicles is readily applied to cell membranes. The results aim at physical-chemical guidelines to optimize the membrane electroporation techniques for the direct transfer of drugs and genes into tissue cells.

Interestingly, there is appreciable efflux of salt ions in the after-field period lasting several seconds. This very important observation suggests that there are not only long-lived open pores but also that the structural basis of the longevity cannot be simple hydrophobic (HO) pores (Figure 1). More complicated higher order structures must have been created by ME, which face higher activation barriers for annealing in the absence of the electric field. A candidate for the higher order structure is the so called hydrophilic (HI) pore. In this sense, ME can hardly be called a breakdown phenomenon. Rather, the reorganization of the lipids in the pore wall leads to a local cluster structure defining an aqueous pore which has a larger electric dipole moment, and thus a higher orientational order than the equivalent space of lipids.

Electroporative transport of drugs and genes

Contrary to the electroporative transport of small salt ions, the transport kinetics of larger macromolecules such as drug-like dyes and DNA, reflects transient interactions with larger pores. The pore size seems to indicate the size of the macromolecule or parts of it which are transiently located within the membrane during the transport process. For instance, the mean pore radius $\bar{r}_p = 1.2 \pm 0.1$ nm, derived from the analysis of the transport of the drug-like dye Serva blue G (SBG), appears to be rather large, although it is in line with previous estimates of possible pore sizes.[15] An open pore of this size should lead to a significant increase in the transmembrane conductivity, reducing locally the transmembrane voltage,[16] eventually causing leakage of cell components and finally cell death. It should be noted that the detection of the dye-permeable pore state is only possible when the dye molecules are (interactively) passing through the pore (Figure 4). There-

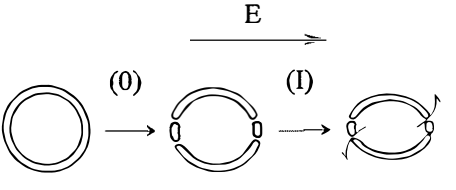

Figure 3. Sequence of events in the electromechanical deformation of a membrane system of unilamellar lipid vesicles or biological cells. Phase 0: Fast (μs) membrane electroporation rapidly coupled to electroporative deformation at constant volume and slight (0.01 – 0.3%) increase in membrane surface area. Phase I: Slow (ms – min) electromechanical deformation at constant membrane surface area and decreasing volume due to efflux of the internal solution through the electropores.

fore, the pore is temporarily occluded by the dye molecule, reducing the conductivity for small ions compared with a dye-free pore of the same radius. Similar arguments apply for the leak pores associated with the transport of DNA.[24,25]

Dye uptake by mouse B cells

As an example for the transport of dye-like drugs, the color change of electroporated intact FcγR⁻ mouse B cells (line IIA1.6) after direct electroporative transfer of the dye SBG (M_r 854) into the cell interior is shown to be prevailingly due to diffusion of the dye *after* the electric field pulse. Hence, the dye transport is described by the First Fick's law where, as a novelty, time-integrated flow coefficients were introduced.[23] The chemical-kinetic analysis suggests three different pore states (P) in the reaction cascade ($C \rightleftharpoons P_1 \rightleftharpoons P_2 \rightleftharpoons P_3$) to model the sigmoid kinetics of pore formation as well as the biphasic pore resealing. The rate coefficient for pore formation k_p is dependent on the external electric field strength E and pulse duration t_E. At E = 2.1 kV cm^{-1} and t_E = 200 μs, $k_p = 2.4 \pm 0.2 \times 10^3\ s^{-1}$ at T = 293 K; the respective (field-dependent) flow coefficient and permeability coefficient are $k_f^0 = 1.0 \pm 0.1 \times 10^{-2}\ s^{-1}$ and $P^0 = 2$ cm s^{-1}, respectively.

The maximum value of the fractional surface area of the dye-conductive pores is 0.035 ± 0.003 % and the maximum pore number is $N_p = 1.5 \pm 0.1 \times 10^5$ per average cell. The diffusion coefficient for SBG, $D = 10^{-6}\ cm^2\ s^{-1}$, is slightly smaller than that of free dye diffusion indicating transient interaction of the dye with the pore lipids during translocation. The mean radii of the three pore states are $\bar{r}(P_1) = 0.7 \pm 0.1$ nm, $\bar{r}(P_2) = 1.0 \pm 0.1$ nm, $\bar{r}(P_3) = 1.2 \pm 0.1$ nm, respectively. The resealing rate coefficients are $k_{-2} = 4.0 \pm 0.5 \times 10^{-2}\ s^{-1}$ and $k_{-3} = 4.5 \pm 0.5 \times 10^{-3}\ s^{-1}$, independent of E. At zero field, the overall equilibrium constant of the pore states (P) relative to closed membrane states (C) is $K_p^0 = [(P)] / [C] = 0.02 \pm 0.002$, indicating 2.0 ± 0.2 % water associated with the lipid membrane.[23]

Finally, the results of SBG cell coloring and the new analytical framework may also serve as a guideline for the optimization of the electroporative delivery of drugs which are similar in structure to SBG, for instance, bleomycin successfully used in the new discipline of electrochemotherapy.[7]

Kinetics of DNA uptake by yeast cells

In a detailed kinetic study it was found that the direct transfer of plasmid DNA (YEp 351, 5.6 kbp, supercoiled, $M_r \approx 3.5 \cdot 10^6$) by

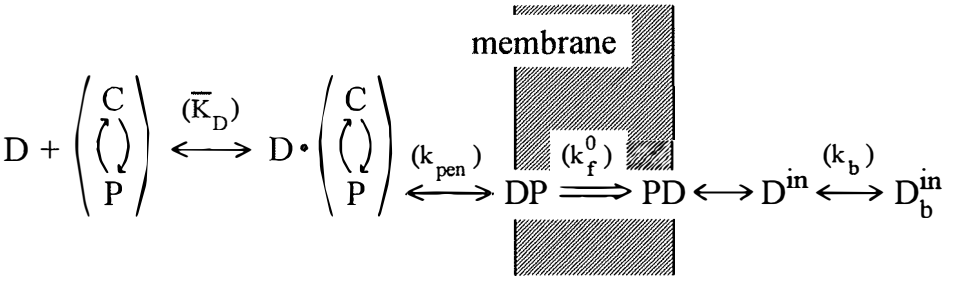

Figure 4. Scheme for the coupling of the binding of a macromolecule (D), either a dye-like drug or DNA (described by the equilibrium constant $\bar{K}_D$ of overall binding), electrodiffusive penetration (rate coefficient k_{pen}) into the outer surface of the membrane and translocation across the membrane, in terms of the Nernst-Planck transport coefficiant (k_f^0) ; and the binding of the internalized DNA or dye molecule (D^{in}) to a cell component b to yield the interaction complex D • b as the starting point for the actual genetic cell transformation or cell coloring, respectively.

membrane electroporation of yeast cells (*Saccharomyces cerevisiae*, strain AH 215) is basically due to (electro)diffusive processes.[26] The rate-limiting step for the cell transformation, however, is a bimolecular DNA binding interaction in the cell interior. Both the adsorption of DNA, directly measured with ^{32}P-dC DNA, and the number of transformants are collinearly enhanced with increasing total concentrations $[D_t]$ and $[Ca_t]$ of DNA and of Ca^{2+} , respectively. At $[Ca_t]$ = 1 mM, the half-saturation or equilibrium binding constant is $\overline{K}_D$ = 15 ± 1 nM at 293 K (20°C). The optimal transformation frequency is TF_{opt} = 4.1 ±0.4 × 10^{-5} if a single exponential pulse of initial field strength E_0 = 4 kV cm^{-1} and decay time constant τ_E = 45 ms is applied at $[D_t]$ = 2.7 nM and 10^8 cells in 0.1 ml. The dependence of TF on $[Ca_t]$ yields the equilibrium constants K^0_{Ca} = 1.8 ± 0.2 mM (in the absence of DNA) and $K^{'}_{Ca}$ = 0.8 ± 0.1 mM (at 2.7 nM DNA) well comparable with K^0_{Ca} = 2.3 ± 0.2 mM and $K^{'}_{Ca}$ = 1.0 ± 0.1 mM derived from electrophoresis data.[26]

In yeast cells, too, the appearance of a DNA molecule in its whole length in the cell interior is clearly an after-field event. At E_0 = 4.0 kV cm^{-1} and T = 293 K, the flow coefficient of DNA through the porous membrane patches is $k^0_f = 7.0 \pm 0.1 \times 10^3 s^{-1}$ and the electrodiffusion (D) of DNA is about 10 times more effective than simple diffusion (D_o): the diffusion coefficient ratio is $D / D_o \approx 10.3$. The mean radius of these pores is r_p = 0.39 ± 0.05 nm and the mean number of pores per cell (diameter 5.5 μm) is $N_p = 2.2 \pm 0.2 \times 10^4$. The maximum membrane area which is involved in the electrodiffusive penetration of adsorbed DNA into the outer surface of the electroporated cell membrane patches is only 0.023 ± 0.002 % of the total cell surface. The surface penetration is followed either by further electrodiffusive, or by passive (after field) diffusive, translocation of the inserted DNA into the cell interior.

For practical purposes of optimum transformation efficiency, 1 mM Ca^{2+} is necessary for sufficient DNA binding and the relatively long pulse duration of 20 – 40 ms is required to achieve efficient electrodiffusive transport across the cell wall and into the outer surface of electroporated cell membrane patches.

Acknowledgments

We thank the Deutsche Forschungsgemeinschaft for grant Ne 227/9-2 to E. Neumann.

References

1. Neumann E, Rosenheck K. Permeability changes induced by electric impulses in vesicular membranes. *J Membrane Biol* 1972; **10:** 279-90.

2. Wong TK, Neumann E. Electric field mediated gene transfer. *Biophys Biochem Res Commun* 1982; **107:** 584-7.

3. Neumann E, Schaefer-Ridder M, Wang Y, Hofschneider PH: Gene transfer into mouse lyoma cells by electroporation in high electric fields. *EMBO J* 1982; **1:** 841-5.

4. Neumann E, Gerisch G, Opatz K. Cell fusion induced by electric impulses applied to dictyostelium. *Naturwissenschaften* 1980; **67:** 414-5.

5. Mouneimne Y, Tosi PF, Gazitt Y, Nicolau C. Electro-insertion of xenoglycophorin into the red blood cell membrane. *Biochem Biophys Res Commun* 1989; **159:** 34-40.

6. Pliquett U, Zewert TE, Chen T, Langer R, Weaver JC. Imaging of fluorescent molecule and small ion-transport through human stratum-corneum during high-voltage pulsing-localized transport regions are involved. *Biophys Chem* 1996; **58:** 185-204.

7. Mir LM, Orlowski S, Belehradek JJr, Teissie J, Rols MP, Serša G, Miklavčič D, Gilbert R, Heller R. Biomedical applications of electric pulses with special emphasis on antitumor electrochemotherapy. *Bioelectrochem Bioenerg* 1995; **38:** 203-7.

8. Tönsing K, Kakorin S, Neumann E, Liemann S, Huber R. Annexin V and vesicle membrane electroporation. *Eur Biophys J* 1997; **26:** 307-18.

9. Seifert U, Lipowsky R. Morphology of Vesicles. In Lipowsky R, Sackmann E, ed. *Structure and Dynamics of Membranes 1A.* Amsterdam: Elsevier; 1995: 403-63.

10. Kakorin S, Redeker E, Neumann E. Electroporative deformation of salt filled lipid vesicles. *Eur Biophys J* 1998; **27:** 43-53.

11. Winterhalter M, Klotz K-H, Benz R, Arnold WM. On the dynamics of the electric field induced breakdown in lipid membranes. *IEEE Trans Ind Appl* 1996; **32:** 125-8.

12. Chang C. Structure and dynamics of electric field-induced membrane pores as revealed by rapid-freezing electron microscopy. in Chang C, Chassy M, Saunders J, Sowers A. ed. *Guide to electroporation and electrofusion.* San Diego: Academic Press, 1992: 9-28.

13. Hibino M, Itoh H, Kinosita K. Time courses of cell electroporation as revealed by submicrosecond imaging of transmembrane potential. *Biophys J* 1993; **64:** 1789-800.

14. Weaver JC. Molecular-basis for cell-membrane electroporation. *Annals of the New York Academy of Sciences* 1994; **720:** 141-52.

15. Weaver J, Chizmadzhev Yu. Theory of electroporation: A review. *Bioelectrochem Bioenerg* 1996; **41:** 135-60.

16. Neumann E, Kakorin S. Electrooptics of membrane electroporation and vesicle shape deformation. *Curr Opin Colloid Interface Sci* 1996; **1:** 790-9.

17. Kakorin S, Stoylov SP, Neumann E. Electro-optics of membrane electroporation in diphenylhexatriene-doped lipid bilayer vesicles. *Biophys Chem* 1996; **58:** 109-16.

18. Neumann E. Chemical electric field effects in biological macromolecules. *Prog Biophys molec Biol* 1986; **47:** 197-231.

19. Abidor IG, Arakelyan VB, Chernomordik LV, Chizmadzhev YA, Pastuchenko VP, Tarasevich MR. Electric breakdown of bilayer lipid membrane. I. The main experimental facts and their theoretical discussion. *Bioelectrochem Bioenerg* 1979; **6:** 37-52.

20. Neumann E. The Relaxation Hysteresis of Membrane Electroporation. In: Neumann E, Sowers AE, Jordan C, eds. *Electroporation and Electrofusion in Cell Biology.* New York: Plenum Press, 1989: 61-82.

21. Kakorin S, Neumann E. Kinetics of electroporation deformation of lipid vesicles and biological cells in an electric field. *Ber Bunsenges Phys Chem* 1998; **102:** 1-6.

22. Steiner U, Adam G. Interfacial properties of hydrophilic surfaces of phospholipid films as determined by method of contact angles. *Cell Biophysics* 1984; **6**: 279-99.

23. Neumann E, Toensing K, Kakorin S, Budde P, Frey J. Mechanism of electroporative dye uptake by mouse B cells. *Biophys J* 1998; **74:** 98-108.

24. Spassova M, Tsoneva I, Petrov AG, Petkova JI, Neumann E. Dip patch clamp currents suggest electrodifusive transport of the polyelectrolyte DNA through lipid bilayers. *Biophys Chem* 1994; **52:** 267-74.

25. Hristova NI, Tsoneva I, Neumann E. Sphingosine-mediated electroporative DNA transfer through lipid bilayers. *FEBS Lett* 1997; **415:** 81-6.

26. Neumann E, Kakorin S, Tsoneva I, Nikolova B, Tomov T. Calcium-mediated DNA adsorption to yeast cells and kinetics of cell transformation. *Biophys J* 1996; **71:** 868-77.